Available online at www.sciencedirect.com
SCIENCE DIRECT®

Journal of the European Ceramic Society 23 (2003) 81–89

www.elsevier.com/locate/jeurceramsoc

# Subcritical crack growth in $Al_2O_3$ with submicron grain size

Andreas Krell[a,*], Eckhard Pippel[b], Jörg Woltersdorf[b], Wolfgang Burger[c]

[a]*Fraunhofer Institute of Ceramic Technologies and Sintered Materials (IKTS), Winterbergstrasse 28, D-01277 Dresden, Germany*
[b]*Max-Planck-Institute of Microstructural Physics, D-06120 Halle (Saale), Germany*
[c]*CeramTec AG - Innovative Ceramic Engineering, D-73207 Plochingen, Germany*

Received 15 November 2001; received in revised form 22 February 2002; accepted 3 March 2002

**Abstract**

Gelcast sintered $\alpha$-$Al_2O_3$ (corundum) ceramics were developed with a sub-μm grain size at densities >99%. Highly perfect samples with a minimum of flaws were prepared by an approach that maintains the high purity of the raw powder >99.99% $Al_2O_3$ throughout processing. As a consequence, all grain boundaries are free of even thinnest amorphous interface films, amorphous triple junctions are ⩽150 nm, and their frequency is low. Subcritical crack growth was investigated by an approach recording growth rates as low as $10^{-13}$ m/s. The outstanding purity of grain boundaries gives rise to a resistance against subcritical crack growth which is similar or even below that of coarser conventional alumina ceramics. No significant promotion of subcritical crack growth by water was observed for the new gelcast high-purity ceramics with grain sizes <1 μm, and there is no indication of a threshold $K_{I0}$ below which no crack growth would occur. The results suggest that in sintered alumina ceramics with a given purity of grain boundaries the subcritical crack-growth mechanism of stress corrosion is independent of the grain size. With their high mechanical reliability, these corundum grades are promising candidates for the use in new prostheses for joints with a high load bearing capability and with small calliper sizes. 

*Keywords:* $Al_2O_3$; Bioceramics; Grain boundary engineering; Stress corrosion; Subcritical crack growth

## 1. Introduction

Components of high purity sintered alumina ceramics for use in aqueous media have been produced for several decades. Known examples are ball-heads in artificial hip joint prostheses and dense alumina membranes in pressure sensors. Remarkable progress in terms of further improvements in the wear resistance[1] and strength[2] was achieved during the past ten years by the development of microstructures with grain sizes <1 μm.

Manufacturing of these ceramics requires increasingly fine-grained powders the compaction of which, however, is rather difficult. To minimise the size and frequency of defects, *liquid shaping* procedures starting from suspensions are attractive. The mechanical properties of high purity alumina have been improved significantly associated with both the availability of new grades of highly pure, chemically synthesised powders and with new shaping approaches that enable a more homogeneous co-ordination of extremely fine-grained powder particles, reduce the sintering temperature and provide, finally, dense microstructures with sub-μm grain sizes.[2]

Another motivation to develop new shaping technologies arises when components with more complex shapes are required (e.g. for a ceramic knee prosthesis). Whereas the microstructures provided by the new approach are known to exhibit improved wear[1] and strength properties,[2] little is known about the long-term reliability of these materials. For example, slow (subcritical) crack growth is known to proceed preferentially along the grain boundaries where crack growth rates are much higher than within a perfect crystal lattice. With the increased frequency of grain boundaries in sub-μm ceramics and regarding the importance of this feature for the reliability of the components, it was the objective of the present work to investigate the influence of the grain size and of the state of grain boundaries (depending, e.g., on doping additives) on the subcritical crack growth in different environments.

Besides the interest in new materials there is also a need of additional testing approaches able to assess very

* Corresponding author. Tel.: +49-351-2553-538; fax: +49-351-2553-600.
*E-mail address:* andreas.krell@ikts.fhg.de (A. Krell).

0955-2219/02/$ - see front matter 
PII: S0955-2219(02)00072-9

Table 1
Microstructural and mechanical properties of investigated materials

| Grade | Dopant (wt.%) | Relative density (%) | Average grain size (μm) | Vickers hardness (HV10) | Fracture toughness $K_{Ic}$ (MPa$\sqrt{m}$) | Strength (3-pt-bending) (MPa) |
|---|---|---|---|---|---|---|
| GC63 | 0 | 99.1 | 0.8 | 2030 | 3.9 | 783±76 |
| GC90E | +0.1% MgO | 99.3 | 0.6 | 2100 | 3.3 | 737±56 |
| Uniaxially dry pressed | +0.65% $ZrO_2$ | 99.8 | 1.25 | 1760 | 3.5 | 400±60 |
| Commercial reference | +MgO | 99.8 | 4–6 | 1780 | 3.6 | 598±33 |

low crack propagation rates $v$. At low driving force (stress intensity) $K_I$, a power law

$$v = AK_I^n \quad (1)$$

is commonly assumed with a parameter A, and $K_{I0}$ defines a $K_I$ threshold below which no crack propagation occurs. Obviously, it would provide a clear technical benefit to find a perfectly safe region of operation at $K_I < K_{I0}$. This, however, is not easy because the involved crack velocities of sintered alumina are very low (at least in the region of $10^{-11} \ldots 10^{-10}$ m/s which is the lower limit of double torsion tests[3,4]). To overcome this lack of experimental data, Fett and Munz[5] have analysed static fatigue (strength) data up to 500 h and derived $v$-$K_I$ curves down to $10^{-12}$ m/s. Again based on long-time studies, a more simple approach was applied here to assess similarly low crack propagation rates without occupying strength testing devices for such a long time.

## 2. Experimental procedure

### 2.1. Sample preparation

The preparation of the materials was described previously.[2] Aqueous gelcasting slurries were prepared from an 0.2 μm corundum powder (TM-DAR, Boehringer Chemicals, Japan; purity >99.99%) with an additive of a polymerisable monomer. Some of the microstructures were doped with 0.1% MgO (Table 1). To avoid any contamination from wear of grinding balls, the slurries were prepared by stirring assisted by ultrasonification. After homogenisation, an initiator was added and shaped samples were obtained by directly casting the slurry into a mould where consolidation occurs by polymerisation of the organic binder. The components were then demoulded, dried, sintered for 2 h in air and ground.

Fig. 1 gives typical microstructures, Table 1 presents some microstructural and mechanical data. The density was obtained by Archimedes' principle and related to a theoretical density of 3.9865 g/cm$^3$, the grain size is given as the linear intercept length multiplied by 1.56.[6] The Vickers hardness was measured at a testing load of 10 kgf (98.1 N) with a dwell time of 30 s, the fracture toughness was derived from indentation techniques (direct crack length measurement [Eq. (2) below] confirmed by indentation-strength in bending). For strength measurements, the span length in 3-point-bending was 30 mm, the cross head velocity 0.5 mm/min. Additional tests in 4-point-bending with standard 20/40 mm span

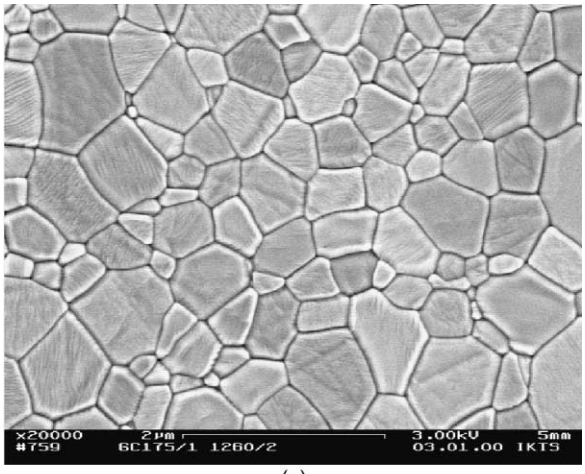

(a)

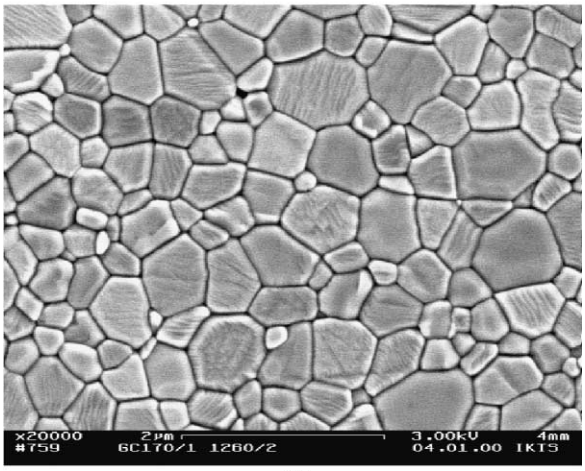

(b)

Fig. 1. (a) Undoped gelcast $Al_2O_3$, sintered at 1260 °C. Average grain size 0.75 μm. (b) MgO-doped gelcast $Al_2O_3$, sintered at 1260 °C. Average grain size 0.63 μm.

revealed a strength of 600–650 MPa (±65 MPa) for the gelcast sintered bars.

An analysis of flaws in gelcast specimens revealed that fracture of low-strength samples (local stress at origin <600 MPa) was initiated by pores (diameter >50 μm) in the volume of the microstructures, whereas the fracture of stronger bars started from small (probably grinding induced) crack near the surfaces.[7] To investigate the effect of different flaw distributions, additional samples were prepared from the same powder by uniaxial pressing (200 MPa). Due to the less homogeneous compaction, these samples required a high sintering temperature of 1450 °C for a relative density >99% (gelcasting: 1260–1280 °C!). As a consequence, their 3-point-bending strength was 400 MPa compared with about 800 MPa observed for the gelcast bodies.[2]

### 2.2. Electron microscope examination

Thin specimens were prepared for transmission electron microscopy (TEM) by cutting thin slices (<200 μm), dimple-grinding to about 10 μm, and final Ar-ion milling. This enables the desired high resolution investigation of specimen areas with a thickness of a few nanometers and with a tolerable surface roughness.

Using the high resolution Philips CM 20 FEG field emission electron microscope (HREM), run at 200 kV, the microstructure of grain boundaries without or with amorphous phases could be imaged down to the atomic range. The chemical composition near the grain boundaries and at individual amorphous grain triple junctions was estimated by energy dispersive X-ray spectroscopy (EDXS) with a nanometer resolution (Tracor-Voyager II detector system attached to the CM 20 microscope, operated in the scanning mode).

### 2.3. Measurement of subcritical crack growth

Subcritical crack growth in an aqueous environment has to be minimised when a high strength of reliable components shall be guaranteed for a long period of use. To avoid inaccuracies from long-range extrapolations, the testing procedure should be able to record very small rates of crack growth at low driving stress intensities $K_I$. When subcritical crack growth data are obtained from an investigation of the time-dependent growth of indentation cracks, the driving force is the residual stress at the indentation site which does not relax on unloading (plastic recovery is insignificant in this highly brittle material, and elastic stress relief from crack growth is considered small with the small increase of the crack lengths reported below for $t=5$ min→6 months). Very small growth rates can be recorded and reliable data on the long-time behaviour are obtained without extensive extrapolation when the crack length is measured over several months.[2] The value of *starting data* in such investigations is, however, limited when significant subcritical growth occurs immediately after unloading before the first optical measurement of a crack length can start. It was, therefore, recommended to use this method preferentially for *long periods* of growth (weeks → months), where the influence of the starting inaccuracy is small.[2]

With an indentation load of $F=98.1$ N (10 kgf), the typical crack lengths $2c$ at $t_0 \approx 5$ min are about 380–450 μm; after 6 months, they have grown up to 430–520 μm. These cracks are "short" compared with the crack length in precracked bending bars but large compared with the typical flaw sizes in high-strength ceramics.[7] In the fine-grained ceramics investigated here, R-curve effects are improbable, but, nevertheless, no final information on the equivalence of the present results with the subcritical growth of *shorter* flaws is available, and any interpretation should be done with care.

When the subcritical crack growth rate $v$ is given by the slope $dc/dt$ at time $t$, the usual presentation of the subcritical rate $v$ depending on the stress intensity $K_I(c)$ in a $K_I$-$v$ plot requires to associate the observed crack length $c(t)$ (at a driving force induced by the Vickers load $F=98.1$ N) with $K_I(c)$ active at a distance $c$ from the centre of the indent. It was assumed here that this stress intensity $K_I(c)$ can be calculated by one of the equations derived to describe the relationship between the length of indentation cracks and the fracture toughness $K_{Ic}$. The relationship

$$K_{I(c)} = \S_V{}^R \cdot (E/H)^{1/2} \cdot \left(F/c^{3/2}\right) \quad (2)$$

originally derived by Anstis et al.[8] incorporates the Young's modulus $E$ and the Vickers hardness $H$ [approximately independent of load when measured at a sufficiently large testing load, e.g. as HV10 (Table 1)]. For the empirical parameter $\S_V{}^R$ a value of 0.023 was used here as it can be derived for $Al_2O_3$ ceramics from calibrating investigations (Fig. 5 in Ref. 8).

For measurements in distilled water special care was taken to avoid scattering results originating from a limited wettability of specimen surfaces[9] or from the difficult penetration of the liquid into narrow cracks.[10] The indentation process was, therefore, conducted in water avoiding any primary contamination of the generated crack surfaces with air molecules. At the beginning of crack formation and depending on the velocity of water diffusion on crack surfaces, this procedure per se does not exclude a real crack tip situation as in a vacuum. However, in water the typical crack growth rate at the beginning of stage II (where increasing $K_I$ does not further increase the crack velocity because of the slower diffusion of water molecules) is $\geqslant 10^{-4}$ m/s for sapphire and sintered alumina[3,11,12] indicating a diffusion rate of water on crack surfaces in the range of 100 μm/s. It is, therefore, suggested here that already the first measurement of

crack lengths (5 min after indentation) addressed indentation cracks which where completely occupied by diffused water.

## 3. Results

### 3.1. Characterisation of grain boundaries

High resolution electron microscopy was used for elucidating the influence of the grain boundary structure on subcritical crack growth. The existence of glassy phases along grain boundaries and in triple junctions was of particular interest in these investigations since subcritical crack growth is known to proceed much faster in glasses of any composition[13] than in single crystalline $Al_2O_3$ (independent of the orientation[11,14,15]).

Fig. 2 shows a typical HREM image of a grain boundary in high-purity gelcast $Al_2O_3$ prepared from TM-DAR corundum powder. It can be clearly seen that the atomic planes of adjacent grains directly meet each other without any amorphous material in between.

Whereas such perfect boundaries can also be found in most other corundum ceramics, the difference is that conventional grades exhibit a neighbourhood of both "clean" boundaries and triple junctions which are filled with glass and where this amorphous phase frequently enters parts of the adjacent boundaries.[16] With the technology used for the preparation of the new high-purity grades investigated here, however, the purity of the raw powder is maintained throughout the whole process. As a consequence, no one amorphous grain boundary film was observed.

The frequency of amorphous triple junctions is very small, and the size of these few defects is typically $\leqslant 150$ nm (Fig. 3). As expected, an EDX line scan revealed some local Si enrichment at the position of the amorphous triple junction. It should be noted that these Si-containing triple junctions are also observed when the same high-purity powder is processed by other approaches (e.g. by pressure filtration); i.e. the silicon impurity is not a relict of the specific organic additives used in gelcasting.

Although some triple junctions contain amorphous material this never extends into the neighbouring grain boundaries of the ceramics investigated here. This feature (typical for $Al_2O_3$[16] boundaries and also for advanced $ZrO_2$[17]) is exemplified by the HREM image of Fig. 4: while most of the triple area (upper right) is amorphous, the boundary between the two adjacent alumina grains is completely free of amorphous material (lower left).

### 3.2. Crack growth observations

Fig. 5 displays the results of crack length measurements in air and in water at ambient conditions. Note that the shorter crack length of the undoped sub-μm gelcast sample (GC63 in Table 1) is just an evidence of its slightly larger *critical* stress intensity $K_{Ic}$ given in Table 1. The *subcritical* performance, however, is characterised by its change with time at the driving stress intensity $K_I$ defined by Eq. (2).

In the logarithmic-linear $t$-$2c$ plot of Fig. 5, the slope of the curves is similar for all of the investigated microstructures, but it has to be emphasised that this slope

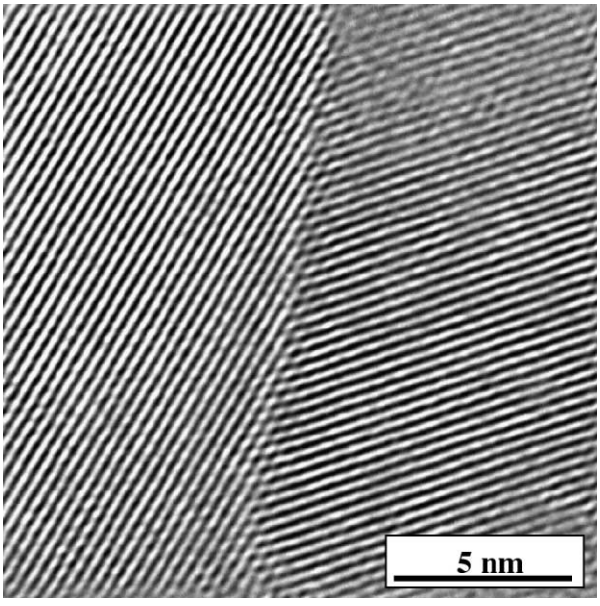


Fig. 2. Typical HREM image of a grain boundary in undoped high-purity gelcast corundum (from TM-DAR powder). The boundary is free of amorphous material or crystalline precipitates.

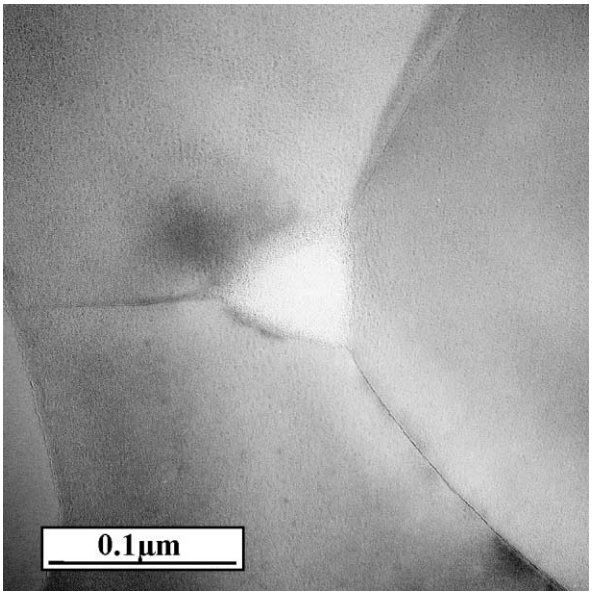


Fig. 3. Small amorphous triple junction in high-purity gelcast corundum ceramics.

gives no immediate information about the subcritical crack growth performance: the linear appearance of the curves implies a growth like

$$dc/dt \sim 1/t \quad (3)$$

which is nothing else than the expected general feature of a crack growth which becomes slower with time because the crack proceeds into more distant (from the centre of the indentation) regions of the driving stress field, then providing lower $K_I$.

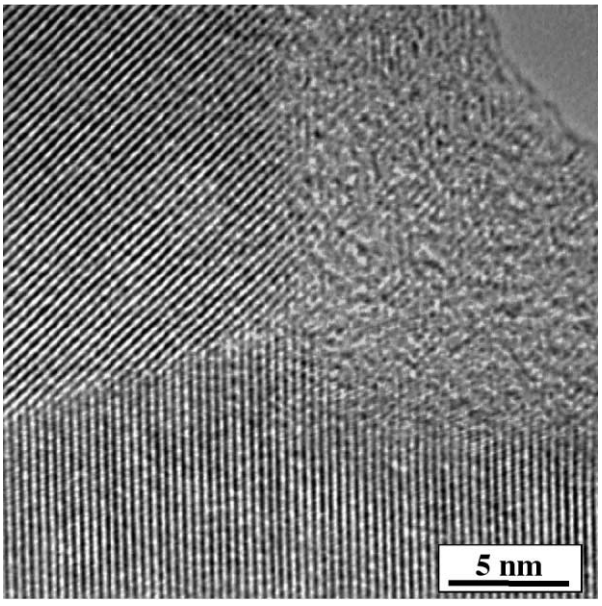


Fig. 4. HREM image of part of a triple junction similar to that of Fig. 3. The adjacent grain boundary is free of amorphous material.

With this understanding, similar growth rates (slopes) at shorter crack lengths $2c$ in Fig. 5 give evidence that after a given time the undoped sub-μm gelcast sample GC63 exhibits a similar subcritical crack velocity *despite a higher driving stress intensity* $K_I$ [Eq. (2)]—the purest microstructure exhibits the highest resistance to subcritical ageing as in air as in water.

Note that Eq. (3) is a purely empirical expression of the *experimental observation* of the kinetics displayed in Fig. 5 and should not be confused with known analytical treatments where $K_I$ terms like Eq. (2) are inserted into the commonly assumed $v$-$K_I$ relationship of Eq. (1) resulting in expressions as

$$dc/dt \sim c^{-3n/2}. \quad (3a)$$

Equations like (3a) cannot provide an information about the kinetics of the crack propagation process and are, therefore, not a substitute for the *experimental result* expressed by Eq. (3).

### 3.3. $K_I$-v *diagrams*

Fig. 6 associates the observed crack growth rates of gelcast sub-μm alumina ceramics in air and in water (from Fig. 5) with the calculated $K_I(c)$. Note that the smallest growth rates $dc/dt$ are as low as $10^{-13}$ m/s here, whereas the lower limit of other approaches is $v \geqslant 10^{-8}$ m/s. The similarity of the present results compared with the data published by Shiono et al.[11] (Chevron notch, 4-point-bending) and by Ebrahimi et al.[12] (double torsion, known as prone to R-curve influences) confirm the general validity of the new

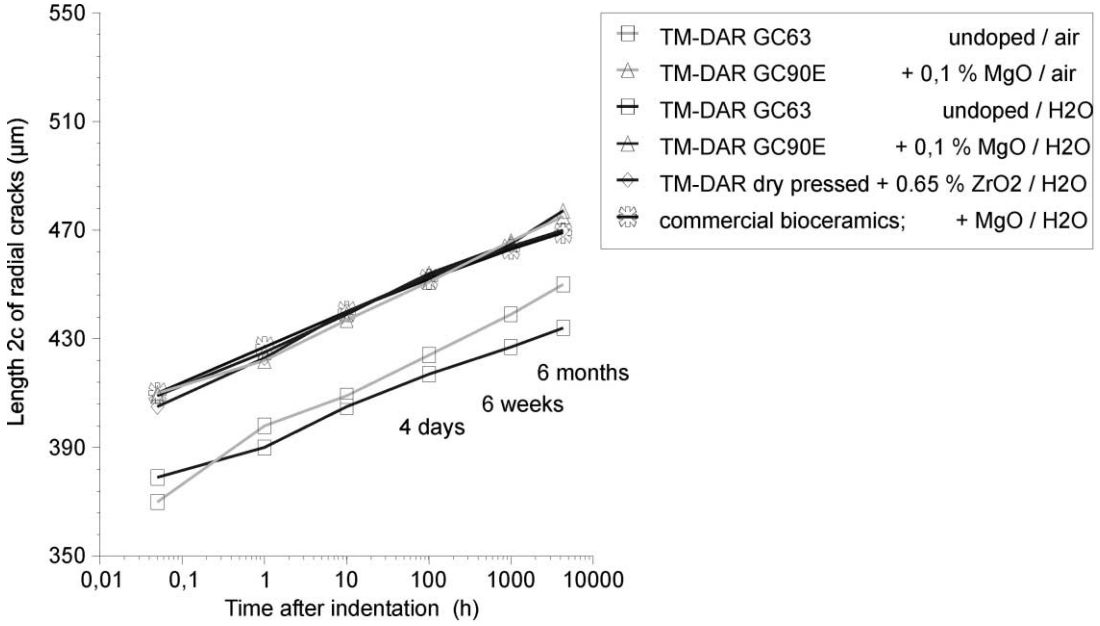


Fig. 5. Development of radial crack length in air and in distilled water. High-purity gelcast sub-μm alumina compared with a uniaxially dry pressed grade and with commercial bioceramics.

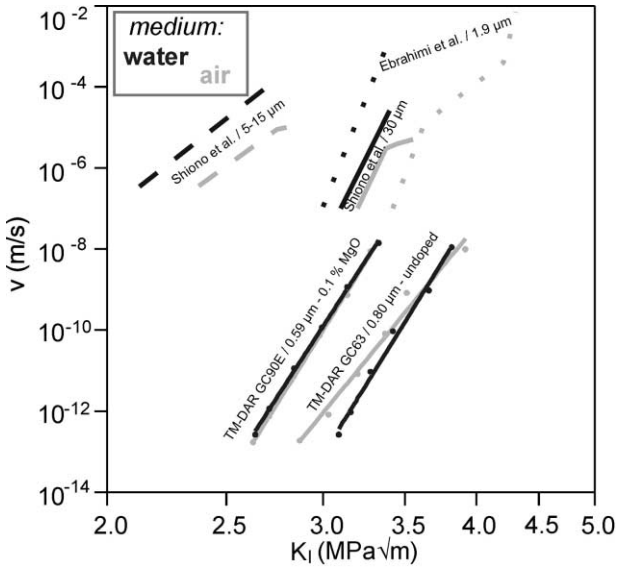


Fig. 6. Subcritical crack velocity of high-purity gelcast sub-µm corundum ceramics in water (bold graphs) and in air (light) compared with data from the literature. The differences between water and air (20 °C) differ for the different ceramics, but apparently they are not influenced by the different values of the relative humidity of 67%,[11] 50%[12] and 40% (present investigation).

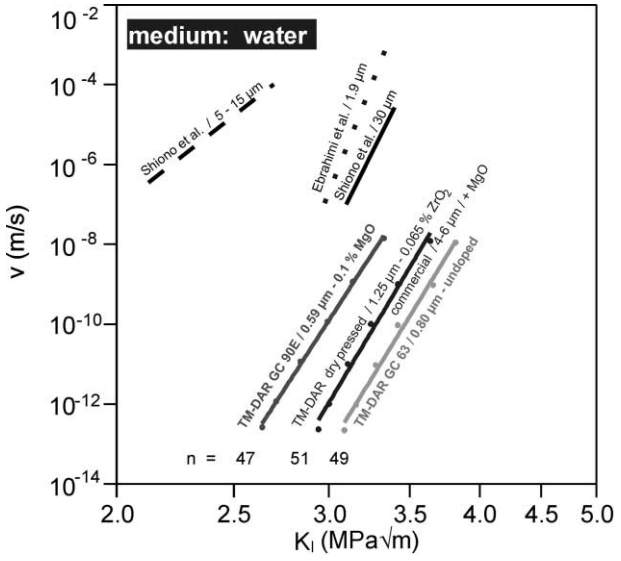


Fig. 7. Subcritical crack velocity of new sub-µm corundum ceramics in water compared with coarser alumina microstructures (one dataset is displayed for the identical behaviour of the commercial reference and the uniaxially dry pressed 1.25 µm sample). The parameter n given for the present results is the exponent from Eq. (1).

approach applied here to record *lower rates* of subcritical crack growth $<10^{-8}$ m/s.

A first important result is that the high-purity sub-µm ceramics prepared and investigated here do not exhibit a significant influence of water on the crack length at the low crack propagation rates $<10^{-8}$ m/s investigated here. This result is also evident directly from the original crack length data in Fig. 5.

An understanding of the different impact of water on the subcritical crack growth behaviour of the materials in Fig. 6 requires some additional information about their manufacture and microstructure. Little information was provided about purity and flaw distribution of samples investigated by Shiono et al.[11] Ebrahimi et al.[12] produced their sintered ceramics from a powder with a particle size of 0.25–0.30 µm and with a purity of about 99.95% $Al_2O_3$ doped with 0.05% MgO (SM8, Baikowski, France). Whereas the purity should, therefore, have been slightly lower as in the ceramics investigated here, their processing data indicate a larger population of flaws. Cold isostatic pressing at 350 MPa resulted in a relative green density of 55% and in the following sintering performance:

- relative density 99.2%,
- obtained after sintering at 1550 °C and
- associated with a grain size of the sintered microstructure of 1.9 µm.

However, with the *same powder* and a *similar shaping* approach (cold isostatic pressing at, however, 700 MPa), one of the present authors obtained a green density of 59% and greatly improved sintering:

- relative density 99.2%,
- obtained after sintering at only 1450 °C and
- associated with a much finer grain size of the sintered bodies of 1.1 µm.[18]

Since the sintering temperature is a sensitive indicator of the compaction *homogeneity* of fine-dispersed powders,[2] the big difference of 100 °C provides clear evidence of a surplus of defects in the samples investigated by Ebrahimi et al.[12]

Fig. 7 compares the results in water for the different materials presented by Table 1 with data from literature. The most important result is the comparison with conventional (coarser) alumina ceramics investigated by Shiono et al.:[11] whereas known fine-grained ceramics exhibit faster subcritical crack propagation than coarser microstructures[11,19] (because of the preference of the path along grain boundaries at small grain sizes and due to the faster growth along grain boundaries compared with the lattice), Fig. 7 shows no indication of accelerated subcritical crack growth in the (highly pure) sub-µm ceramics. This statement holds *independent* of the preparation (uniaxial dry pressing or gelcasting) and independent of the doping level.

On the other hand, there are obvious differences *between* these fine-grained ceramics: the purest

(undoped) gelcast grade GC63 exhibits the largest resistance to subcritical ageing.

## 4. Discussion

The high strength of the new sub-μm corundum materials prepared by gelcasting (Table 1) gives evidence of the reduced size and frequency of larger flaws in these ceramics where fracture starts at grinding induced flaws of about 20 μm size.[7] The results obtained here for the *subcritical* crack growth resistance, however, are rather surprising:

1. The influence of water.
   Water is known to promote subcritical growth in both *single crystalline* $Al_2O_3$ (sapphire)[14] and in *polycrystalline* alumina ceramics.[3] When Figs. 5 and 6 now indicate no (or, at least, an only minor) influence of water on subcritical growth in doped and undoped *high-purity* gelcast corundum ceramics (highly perfect with a minimum of flaws), it should, on the other hand, be remembered that the *extent* of the effect of water increases ranking from sapphire to coarser alumina and fine grained alumina[11] (strongest impact of water in the finer microstructures, possibly enhanced further by the presence of defects as noted above for the samples investigated by Ebrahimi et al.[12]). This observation implies two options: water promotes subcritical crack growth preferentially
   (i) in the local regions of *lattice disorder* along grain boundaries, and/or
   (ii) in microstructural regions with segregated *impurities* in grain boundaries.
   The present result of a *minor* influence of water on subcritical crack growth in extremely fine grained (sub-μm) but high-purity polycrystals favours the second explanation (ii).

2. The effect of grain size.
   It was repeatedly reported that in conventional alumina ceramics microstructures with grain sizes of about 4–10 μm exhibit faster subcritical crack growth at smaller driving stress intensities $K_I$ (in air) than coarser grades with grain sizes between 20 and 30 μm.[11,19]
   Since glasses of any composition exhibit faster subcritical growth rates than sapphire (of any orientation), again the two reasons (i) and (ii) are possible as outlined above.
   And again the present observation of no deterioration of the subcritical growth resistance in the new sub-μm but high-purity ceramics favours the interpretation, that impurities (segregated in grain boundaries and present as second phase inclusions in triple points) are more detrimental to subcritical ageing than a "pure" atomic disorder along the boundaries. This conclusion is in a fair agreement with the observation of Ebrahimi et al. (on similarly *high-purity* alumina): increasing grain sizes $>2$ μm lead to enhanced crack resistance, but a unique $K_I$-$v$ law is obtained if the R-curve effect is subtracted.[12]

Concluding, the present results suggest that both

- the surprising lack of a significant promotion of subcritical crack growth by water, and
- the observation that the new sub-μm $Al_2O_3$ ceramics exhibit subcritical growth rates similar to or even below those reported for coarser conventional grades have to be attributed to the outstanding purity of the grain boundaries in the new $Al_2O_3$ ceramics.

This general conclusion is further substantiated by the observation that among the ceramics investigated here all *doped* microstructures exhibit slightly *higher* subcritical growth rates than the undoped grade GC63 (Fig. 7).

However, the specific nature of the mechanism *how* doping additives or impurities affect the resistance against subcritical crack growth is not clear at present. The 0.1% MgO doping level in GC90E is well above the limit of solubility at sintering, it is, however, too small to give readily observable second phase particles of MgO or spinel in the alumina microstructure. Nevertheless, *there is* an "active" presence of the MgO dopant throughout sintering (as evidenced by the reduced grain size — cp. Table 1). When, *with* this dopant GC90E exhibits enhanced subcritical crack growth (Fig. 7) *in spite of the absence* of second phase precipitates, this observation may indicate a sensitive response of the subcritical growth resistance to atomic segregation of less than one monolayer.

Whereas the present investigations were intentionally focused to record very small rates of crack growth, additional experiments able to assess higher rates in these sub-μm microstructures are clearly desirable to answer open questions. If, for example, all MgO doped samples in water exhibit slightly higher subcritical growth rates than the undoped grade GC63 (Fig. 7), doping should also induce a stronger effect of water, and even the highly pure undoped grade GC63 should exhibit some influence of water as it is known for pure corundum single crystals. Fig. 6, however, does not reveal such effects, probably because the crack propagation rates assessed by the present approach are too

low: most of the previous investigations comparing subcritical growth of single or polycrystalline $Al_2O_3$ in dry air, wet air or water resulted in similar or identical $K_I$–$v$ curves in these different media at the *low* crack growth velocities $\leqslant 10^{-8}\ldots10^{-6}$ m/s of the "stage I" $v \sim K_I^n$ relationship, and a real difference between dry and wet (aqueous) conditions was often revealed by different rates in the later "stage II" only (i.e. at *higher* crack velocities $>10^{-8}$ m/s).[3,11,14] Such high rates have not been recorded by the present tests and are not displayed, therefore, in Fig. 6.

With crack growth rates in doped gelcast GC90E *beyond* the data of dry pressed samples (uniaxially pressed from TM-DAR, and cold isostatically pressed commercial grade), Fig. 7 suggests a *minor influence of defects* on the subcritical crack resistance for these microstructures. Probably it is the real structure of grain boundaries which is the governing factor in all these high-purity and rather perfect sintered alumina microstructures.

Note that after 6 months of aging in water and with crack propagation rates as low as $10^{-13}$ m/s the results in Fig. 7 *do not* provide any indication of a threshold $K_{I0}$ *neither* for the three high-purity grades with different grain sizes, doping levels and defect populations *nor* for the commercial reference. This observation has to be compared with early[3] and recent results[4] obtained in air with most different aluminas (purities 95% $Al_2O_3$ up to biomedical grade, grain sizes 1.7–25 μm) where *all* reported data down to rates of about $10^{-11}\ldots10^{-10}$ m/s are perfectly on usual $v \sim K_I^n$ lines, and only very few data at still lower velocities[4] have been addressed by the authors as an indication of a static fatigue limit $K_{I0}$. However, these smallest crack velocities have been near or beyond the lower limit of propagation rates that could be assessed by the applied double torsion method. It appears, therefore, that the present and most of the previous data indicate a threshold $K_{I0}$ which—if existent at all—refers to very low rates $\leqslant 10^{-13}$ m/s. Surprisingly, this finding appears to be independent of the grain sizes and the purity.

## 5. Conclusions

Subcritical crack growth was investigated by an approach which enables to record growth rates as low as $10^{-13}$ m/s. These data reduce the extent of extrapolation when lifetime predictions are required to evaluate the long-term ageing behaviour of load bearing ceramics. Down to $10^{-13}$ m/s there was no indication of a threshold $K_{I0}$ neither for the investigated high-purity samples nor for the commercial reference.

Gelcast corundum ceramics for applications in aqueous environments were prepared from a powder with $>99.99\%$ $Al_2O_3$ by an approach that maintains the high purity throughout processing. As a consequence, all grain boundaries are free of even thinnest amorphous interface films, amorphous triple junctions are $<150$ nm, and their frequency is low.

It is probably the outstanding purity of grain boundaries in these new ceramics which gives rise to an improved resistance against subcritical crack growth:

- The sub-μm ceramics with their improved hardness and strength exhibit subcritical growth rates which — at same driving stress intensity $K_I$ — are similar or even below those known for coarser conventional alumina ceramics.
- Contrary to conventional corundum grades, no significant promotion of subcritical crack growth by water was observed for the new gelcast high-purity ceramics with grain sizes $<1$ μm and with a minimum of defects.

The results suggest that—with a given purity of the grain boundaries in sintered alumina ceramics—the subcritical crack-growth mechanism of stress corrosion is independent of the grain size.

## Acknowledgements

This investigation has been funded by the German Ministry for Education and Research under project No. 03N4010.

## References

1. Krell, A., Improved hardness and hierarchic influences on wear in submicron sintered alumina. *Mater. Sci. Eng. A*, 1996, **209**, 156–163.
2. Krell, A. and Blank, P., The influence of shaping method on the grain size dependence of strength in dense submicrometre alumina. *J. Eur. Ceram. Soc.*, 1996, **16**, 1189–1200.
3. Evans, A. G., A method for evaluating the time-dependent failure characteristics of brittle materials — and its application to polycrystalline alumina. *J. Mater. Sci.*, 1992, **7**, 1137–1146.
4. De Aza, A. H., Chevalier, J., Fantozzi, G., Schehl, M. and Torrecillas, R., Crack growth resistance of alumina, zirconia and zirconia toughened alumina ceramics for joint prostheses. *Biomaterials*, 2002, **23**, 937–945.
5. Fett, T. and Munz, D., Determination of v-$K_I$ curves by a modified evaluation of lifetime measurements in static bending tests. *J. Am. Ceram. Soc.*, 1985, **68**, C213–C215.
6. Mendelson, M. I., Average grain size in polycrystalline ceramics. *J. Am. Ceram. Soc.*, 1969, **52**, 443–446.
7. Krell, A., Fracture origin and strength in advanced pressureless-sintered alumina. *J. Am. Ceram. Soc.*, 1998, **81**, 1900–1906.
8. Anstis, G. R., Chantikul, P., Lawn, B. R. and Marshall, D. B., A critical evaluation of indentation techniques for measuring fracture toughness: I, Direct crack measurements. *J. Am. Ceram. Soc.*, 1981, **64**, 533–538.
9. Chevalier, J., Olagnon, C. and Fantozzi, G., Subcritical crack

propagation in 3Y-TZP ceramics: static and cyclic fatigue. *J. Am. Ceram. Soc.*, 1999, **82**, 3129–3138.
10. Steinbrech, R. W. and Schmenkel, O., Crack-resistance curves of surface cracks in alumina. *J. Am. Ceram. Soc.*, 1988, **71**, C271–C273.
11. Shiono, T., Ota, R. and Soga, N., KI-v diagram for single- and polycrystalline α-Al2O3. *J. Soc. Mater. Sci. Jpn.*, 1983, **32**, 1254–1259.
12. Ebrahimi, M. E., Chevalier, J. and Fantozzi, G., Slow crack-growth behavior of alumina ceramics. *J. Mater. Res.*, 2000, **15**, 142–147.
13. Wiederhorn, S. M., In *Fracture Mechanics of Ceramics*, Vol. 2, ed. R. C. Bradt, D. P. H. Hasselman and F. F. Lange. Plenum, New York, 1974, pp. 613–646.
14. Wiederhorn, S. M., Fracture of ceramics, 1969. *National Bureau of Standards Special Publication*, 1969, **303**, 217–241.
15. Michalske, T. A., Bunker, B. C. and Freiman, S. W., Stress corrosion of ionic and mixed ionic/covalent solids. *J. Am. Ceram. Soc.*, 1986, **69**, 721–724.
16. Pippel, E. and Woltersdorf, J., High-voltage and high-resolution electron microscopy studies of interfaces in zirconia-toughened alumina. *Philos. Mag. A*, 1987, **56**, 595–613.
17. Gremillard, L., Epicier, T., Chevalier, J. and Fantozzi, G., Microstructural study of silica-doped zirconia ceramics. *Acta mater*, 2000, **48**, 4647–4652.
18. Krell, A. and Blank, P., 1997, *Potential Raw Materials for Bioceramics*. Unpublished report, IKTS, Dresden.
19. Freiman, S. W., McKinney, K. R. and Smith, H. L., Slow crack growth in polycrystalline ceramics. In *Fracture Mechanics of Ceramics*, Vol. 2, ed. R. C. Bradt, D. P. H. Hasselman and F. F. Lange. Plenum, New York, 1974, pp. 659–676.